

Modeling of a 2-DOF Piezoelectric Micromanipulator at High Frequency Rates through Nonlinear Black-box System Identification

Helon Vicente Hultmann Ayala¹, Micky Rakotondrabe² and Leandro dos Santos Coelho³

Abstract—In the present paper we proceed the data-driven modeling of a two degrees of freedom (2-DOF) piezoelectric micromanipulator through models with the Nonlinear AutoRegressive with eXogenous inputs (NARX) structure and real acquired data. We show the results when the system is excited at high frequencies, aiming towards rapid and precise micropositioning. The order of NARX the models are increased until they satisfy the statistical tests based on higher-order correlations and the multiple correlation coefficients, which are close to unity for both measured outputs. The results herein presented encourage the use of data-driven methods for modeling piezoelectric micromanipulators.

I. INTRODUCTION

Micropositioning deals with positioning that involves sub-micron resolution. Applications of micropositioning are numerous: microassembly and micromanipulation of artificial objects [1], medical exploration [2] and images scanning [3]. An efficient way to carry out micropositioning tasks is to employ smart or active materials as basis of the actuators as they allow a highly resolute displacement [4]. Piezoelectric actuators are among the well appreciated for that because, additionally to the nanometric resolution possible, they have a large force density and a large bandwidth (in excess of kilohertz is possible) and they are easy to integrate in the design since the power required is electrical. In microassembly and micromanipulation applications, cantilevers structured piezoelectric actuators have been successfully used [1],[4]-[6]. Since some years, two degrees of freedom (2-DOF) [7], [8] have been opening the exploration of dexterous tasks.

Beyond the nonlinearities (hysteresis and creep), piezoelectric cantilevered actuators exhibit high Q-factor. Though the bandwidth is large, such high Q-factor finally leads to a settling time (stabilization time) that is strongly high relative to the raise time. In micromanipulation applications, such long stabilization time as well as the large overshoot drastically affect the tasks. Furthermore, in 2-DOF piezoelectric actuators, there are strong-couplings between the positioning axes which lead to a loss of the accuracy of the tasks. Finally, both the high Q-factor and the cross-couplings

could affect the stability of the multi-DOF piezoactuator if they are not considered carefully. Control of the actuators is therefore mandatory. Different works have been carried out in the modeling of 2-DOF piezoelectric cantilevered actuators [7]–[13] for control purpose, but the consideration of the strong-couplings in high frequency were not fully explored. Consequently, the used models are often approximated or simplified which make necessary the use of robust control techniques with high orders [14]. In addition, such models can not be used to synthesize feedforward controllers which have the advantages of being highly packageable and having low cost [15]. In this paper, we suggest a nonlinear black-box modeling technique and an identification procedure in order to consider strong-couplings in high frequency in 2-DOF piezoelectric actuators. The data-driven models herein presented will provide statistically sound mathematical abstractions to enable better control design and more accurate sensorless control.

The system identification procedure consists in few steps in order to build a model based on measured data, generally for the purpose of control and/or simulation. Many control techniques are model-based, what makes this procedure important in the context of process regulation. Also, for simulation purposes the demand is high, given the complexity of modern processes and the gain in competitiveness simulation offers. Nonlinear black-box system identification offers a general framework to build models capable of capturing nonlinear dynamics phenomena, where nonlinear mappings such as higher order polynomials, artificial neural networks and fuzzy systems are used to construct input-output mathematical relations [16]. In the scope of robotics, in [17] the authors proceed the modeling of an industrial robot through commercially available software for subspace identification. In [18] the authors use system identification procedures in order to estimate inertial and flexibility parameters of an industrial robot. The barycentric parameters of a robot are estimated through computational intelligence techniques in [19]. In [20] the importance of experimental data driven modeling and parameter estimation in robotics are highlighted.

In the present paper the goal is to model the dynamics of the 2-DOF piezoelectric micromanipulator at high frequencies with a two-input two-output (TITO) model. The purpose is to obtain a model for representing the fast dynamics which these devices may achieve. The models which are able to represent rapid dynamics may then be used for design of e.g. model predictive controllers [21], [22] and for simulation. To this end, we measured an input

¹ Helon Vicente Hultmann Ayala is with the Department of Mechanical Engineering at the Pontifical Catholic University of Rio de Janeiro, Brazil and the Industrial and Systems Engineering Graduate Program at the Pontifical Catholic University of Paraná, Brazil. Formerly with IBM Research, Rio de Janeiro, Brazil helon@puc-rio.br

² Micky Rakotondrabe is with the FEMTO-ST Institute, Université Bourgogne Franche-Comté / CNRS, Besançon, France mrakoton@femto-st.fr

³ Leandro dos Santos Coelho is with the Industrial and Systems Engineering Graduate Program, Pontifical Catholic University of Paraná, Brazil, and the Department of Electrical Engineering, Federal University of Paraná, Brazil leandro.coelho@pucpr.br

and output data at high frequencies and built black-box models with different complexities. They were validated by analyzing the properties of the residuals through higher-order cross-correlation based tests, showing the soundness of the approach. modeling 2-DOF piezoelectric devices in high frequencies is a challenging task due to the nonlinear coupling between both degrees of freedom and the hysteretic behavior of the manipulator [23]. The application of the identification procedure to 2-DOF piezoactuators presented in this paper has not been explored in the literature at the best of our knowledge. The approach presented leads to the following advantages: (i) more precise models, which are able to adjust themselves intrinsically to the underlying measured data; (ii) the identification of the hysteresis is made at the same time as the dynamics is captured, which is not the case in traditional modeling of piezoelectric manipulators [24]; and (iii) a unique identification for the multivariable case, which is also not the case in usual works in this domain [4].

The remainder of this paper is organized as follows. Section II gives the equations used for nonlinear black-box system identification in this work. The piezoelectric micromanipulator is detailed in Section III together with the description of the experiment. Section IV exposes the results of the application of the black-box system identification methodology to the 2-DOF micromanipulator and in Section V we give final remarks and future research directions with respect to piezoelectric-based system modeling.

II. NONLINEAR BLACK-BOX SYSTEM IDENTIFICATION

In the following we discuss the system identification procedure, nonlinear structures for autoregressive with exogenous inputs (NARX) models and their validation procedures. The methods herein presented will be applied to model the 2-DOF micromanipulator described in the following section.

The system identification procedure is an iterative and subjective decision making process. It may be summarized in four steps as given below:

- 1) Perform data acquisition: An experiment must be performed in order to get input-output data for the system. The data gathered should be informative enough with respect to the amplitude and frequency band desired to be modeled;
- 2) Define the model: The structure of the model is defined, which in the case of black-box modeling refers to setting the complexity by the choice of the inputs and number of elements;
- 3) Estimate model parameters: Having the data at hand, the input-output pairs are constructed and the parameters are estimated by e.g. some optimization procedure;
- 4) Validate the model: The model should be validated, ideally by analyzing the amplitude and statistical properties of the residuals. Whether it is not validated, one must return to prior steps.

Let us give some notation in order to introduce the class of models used in the scope of the present work. As we here

deal with discrete-time dynamical systems models, the index t refers to the discrete time instants such that $t \in [0, 1, \dots, T_f]$. The i -th output¹ of a multivariable system with I and J inputs and outputs, respectively, is termed as $y_i(t)$, while the j -th output of the system is given by $u_j(t)$. The focus will be on models with the form

$$\hat{\mathbf{y}}(t) = \mathbf{F}[\Phi(t)] \quad (1)$$

with $\mathbf{F}[\cdot]$ as a vectorial nonlinear mapping to the predicted outputs $\hat{\mathbf{y}}(t)$ from $\Phi(t)$, which is the matrix of regressors. Considering the NARX case, we have in $\Phi(t)$ each input and output of the system as

$$\begin{aligned} \Phi(t) = & [y_1(t-1), y_1(t-1), \dots, y_1(t-n_{y_1}), \\ & y_2(t-1), y_2(t-1), \dots, y_2(t-n_{y_2}), \dots, \\ & y_I(t-1), y_I(t-1), \dots, y_I(t-n_{y_I}), \\ & u_1(t-1), u_1(t-2), \dots, u_1(t-n_{u_1}), \\ & u_2(t-1), u_2(t-2), \dots, u_2(t-n_{u_2}), \dots, \\ & u_J(t-1), u_J(t-2), \dots, u_J(t-n_{u_J})], \end{aligned} \quad (2)$$

where n_{y_i} and n_{u_j} are the orders of the i -th and j -th output and input, respectively. In the present work we restrict to the case where each output is given its own nonlinear mapping which depends on its previous values and the inputs of the system

$$\begin{aligned} \hat{y}_i(t) = & F_i[y_i(t-1), y_i(t-2), \dots, y_i(t-n_{y_i}), \\ & u_1(t-1), u_1(t-2), \dots, u_1(t-n_{u_1}), \\ & u_2(t-1), u_2(t-2), \dots, u_2(t-n_{u_2}), \\ & \dots, \\ & u_J(t-1), u_J(t-2), \dots, u_J(t-n_{u_J})]. \end{aligned} \quad (3)$$

Available choices for the nonlinear mapping $F_i[\cdot]$ are e.g. different types of artificial neural networks [25].

In order to estimate the parameters of the model which are present in $\mathbf{F}[\cdot]$, generally the one-step-ahead (OSA) error is used, as it leads to faster parameter estimation algorithms. The OSA prediction is calculated as in (3), by using the most recent amount of measured data. The sole use of the OSA error, however, may be insufficient to assess the quality of a model. It is more adequate to use the free-run (FR) simulation, which amounts to use (3) with past values predicted from the model. In the FR case, measured data is used solely to define the initial conditions of the model. The definition of the residual of the i -th output is

$$\xi_i(t) = y_i(t) - \hat{y}_i(t) \quad (4)$$

where the prediction may be in OSA and FR, according to the type of error one is interested in analyzing. There is a complementary metric called multiple correlation coefficient (R^2) which is defined for the i -th output as [26]

$$R_i^2 = 1 - \frac{\sum_{t=1}^N [\xi_i(t)]^2}{\sum_{t=1}^N [y_i(t) - \bar{y}_i]^2}, \quad (5)$$

¹In general the n -th component of a generic vector v is denoted as v_n .

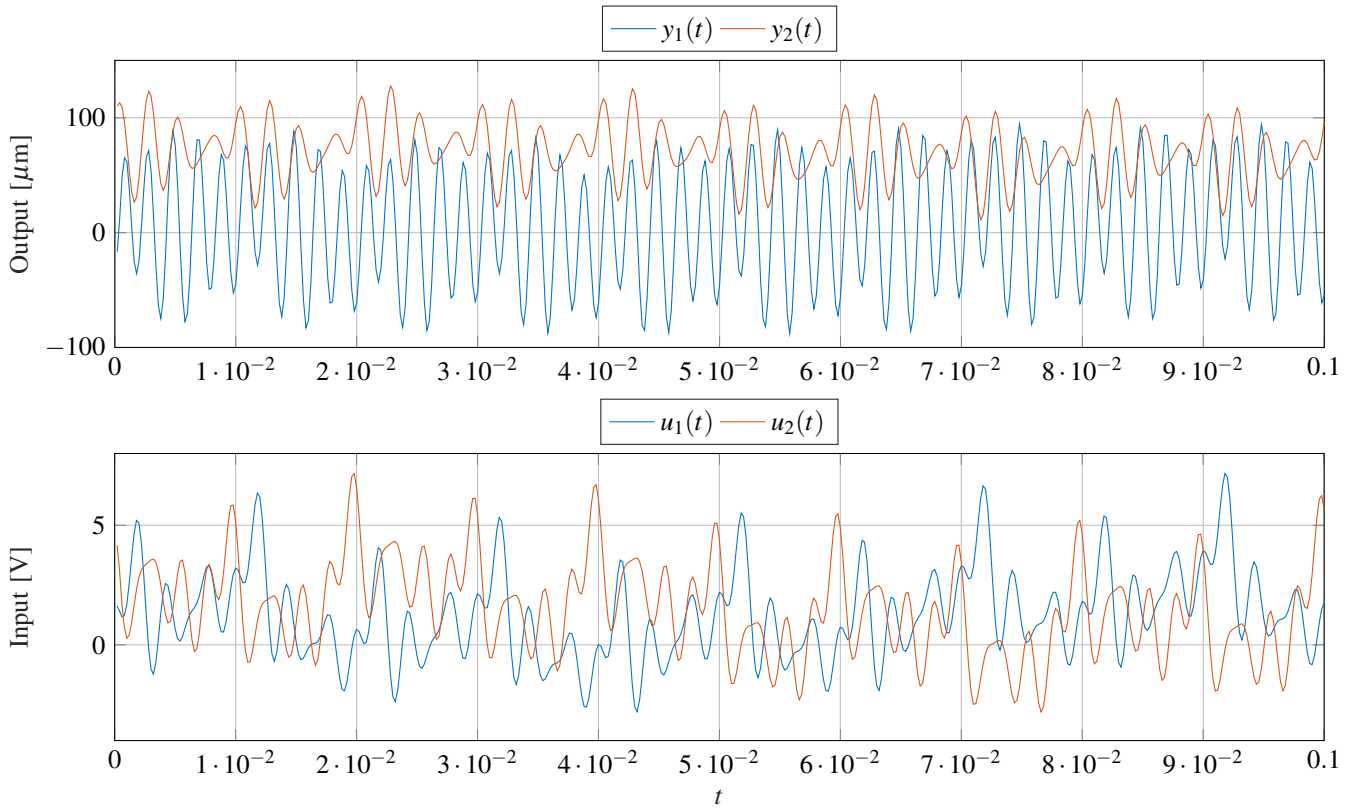


Fig. 1. Exciting signal (lower) and system output (upper) for the 2-DOF micromanipulator.

where \bar{y}_i denotes the mean value of the sequence $y_i(0), y_i(1), \dots, y_i(T_f)$. The R^2 has its maximum value as 1, in the situation that the model has perfectly reconstructed the data.

Detecting the amplitude of the errors is important in order to validate or discard the model depending on the application. A complimentary way to validate the model is the statistical analysis of the residuals, in order to check the randomness of the signal present in the error. The set of tests proposed by [27] can be used, which are based on higher order correlations and also valid for systems on the form (3) for the case of artificial neural networks [28]. It is possible to calculate it between i -th and j -th output and input respectively with

$$\begin{cases} \phi_{\xi_i \xi_i}(\tau) = \delta(\tau), \\ \phi_{u_j \xi_i}(\tau) = 0, & \forall \tau, \\ \phi_{\xi_i(\xi_i u_j)}(\tau) = 0, & \tau \geq 0, \\ \phi_{(u_j^2)' \xi_i}(\tau) = 0, & \forall \tau, \\ \phi_{(u_j^2)' \xi_i^2}(\tau) = 0, & \forall \tau, \end{cases} \quad (6)$$

where $\delta(\cdot)$ is the Kronecker delta function, $(u_j^2)'(t) = (u_j(t))^2 - u_j^2$, $(\xi_i u_j) = \xi_i(t+1)u_j(t+1)$ and ϕ_{ab} is the normalized cross-correlation function between two sequences

$\{a\}$ and $\{b\}$, which is given by [29]

$$\phi_{ab}(\tau) = \frac{\sum_{t=1}^{N-\tau} [a(t) - \bar{a}] [b(t+\tau) - \bar{b}]}{[\sum_{t=1}^N [a(t) - \bar{a}]^2 \sum_{t=1}^N [b(t) - \bar{b}]^2]^{1/2}}. \quad (7)$$

Once the values of the normalized cross-correlation coefficients are calculated for a range of τ in (6), it is possible to infer whether the model adheres to the tests according to the conditions. Commonly, the tests are confronted with a 95% margin as $1.96/(T_f + 1)^{0.5}$, where $T_f + 1$ is the total amount of data.

III. PIEZOELECTRIC MICROMANIPULATOR WITH 2-DOF: CASE STUDY

The present section is devoted to describe the case study, whose measured input and output data are given in Fig. 1. The 2-DOF piezoelectric actuator is presented in Fig. 2a and the different phenomena (e.g. hysteresis and step responses) were explicitly characterized in our previous works [8]. In this paper, the suggested nonlinear black-box model permits to avoid a separated model of each phenomenon, allowing therefore an ease of modeling and identification. When a voltage U_x (resp. U_y) is applied, it bends along the x -axis (resp. y -axis). Unfortunately, there is a residual displacement obtained along the y -axis (resp. x -axis) when U_x (resp. U_y) is applied. This cross-coupling drastically affects the accuracy of the tasks for which the actuator is used. So in the sequel, we consider the actuator as a two-inputs-two-outputs (TITO)

system instead of two single-input-single-output one (see Fig. 2b).

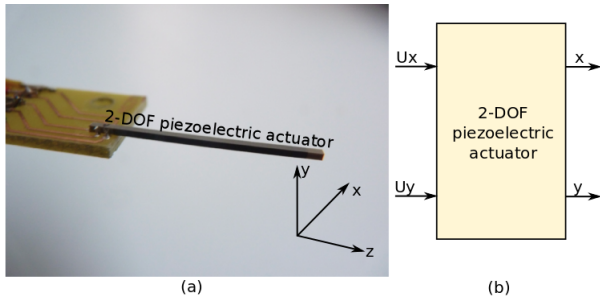


Fig. 2. (a): the 2-DOF piezoelectric actuator. (b): the 2-inputs-2-outputs system.

Figure 3 presents the experimental setup used for the experiments in the rest of the paper. It is composed of (i) the piezoelectric actuator (clamped-free) which has active dimensions of: 25mm x 1mm x 1mm; (ii) two inductive sensors (ECL202 from IBS) measuring the displacement along the x-axis and the y-axis. The sensors are tuned to have a bandwidth of 2kHz and submicron precision; and (iii) a computer and a dSPACE board (DS1103) for the acquisition of the measured displacements and for generating the input voltages.

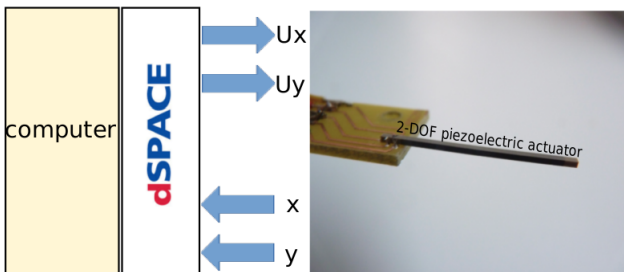


Fig. 3. Diagram of the experimental setup.

Following the notation introduced in (1), the j -th input signal was designed as a multisine with

$$u_j(t) = \sum_{k=1}^{n_f} [A \cdot \cos(2\pi f_k t + \alpha_k)] \quad (8)$$

where n_f is the number of the frequencies of interest, the frequencies are given in Hertz by the vector $\mathbf{f} = [10 \ 50 \ 100 \ 200 \ 300 \ 400 \ 500]$, A is the amplitude set equal for every frequency and α_k random phases for each frequency. We used the inverse Fourier transform to speed up calculations [30]. After this calculation, we scale the signal $u_j(t)$ between $[-5, 5]$ Volts, which is the amplitude of interest. Since the voltage U_x and U_y of the actuator should be within $\pm 10V$, there are no requirements for amplifiers. The input and output pairs are recorded and then used for the purpose of data-driven modeling through system identification methods. The results are depicted in the following.

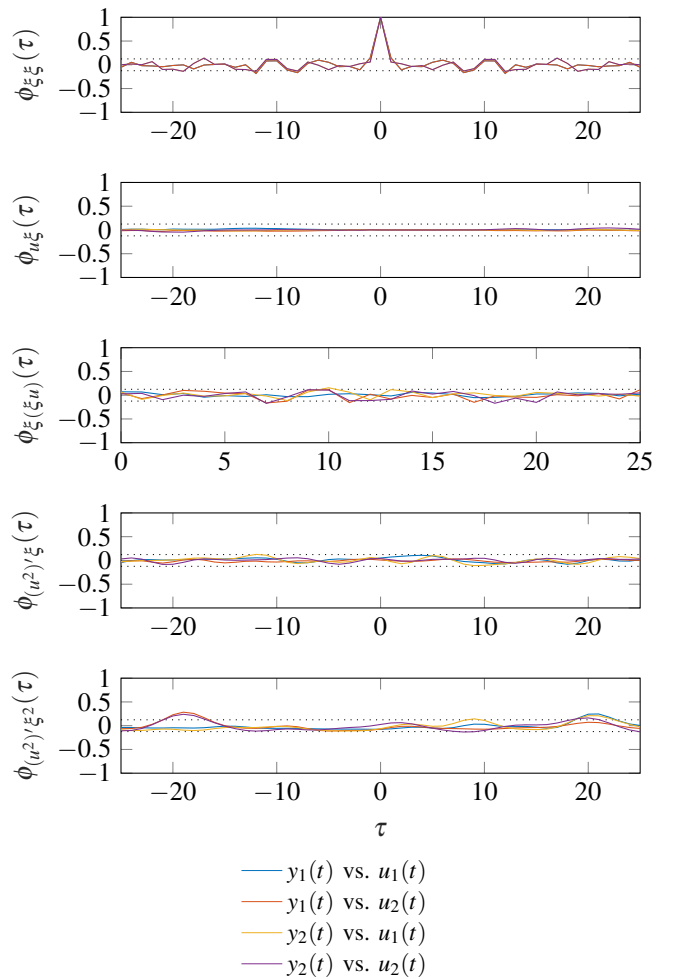


Fig. 4. Correlation tests for the inputs and outputs of the system.

IV. RESULTS

In the present section we describe the results when applying the system identification methodology given in Section II to the 2-DOF piezoelectric micromanipulator described in Section III. We analyze the results in terms of the statistical validation tests based on correlation as in (6) and the R^2 metrics, respectively shown in Figures 4 and 5.

The general NARX model as in Eq. (1) is used to model the TITO system, where the outputs are defined as the displacements in x and y Cartesian axes as respectively $y_1(t)$ and $y_2(t)$ (the same numeration is used for the input signals). As in Eq. (3), we restrict to the case where the models for each output has their own past measurements and both inputs. The reason is to make explicit the cross-couplings among the inputs and outputs of the system. The vectorial nonlinear mapping $\mathbf{F}[\cdot]$ is defined by two artificial neural networks with sigmoidal activation functions, having 6 neurons for each output. We chose such nonlinear mappings due to their well known function approximation capabilities and their complexities where chosen after some trial and error.

The data was acquired with $50 \mu s$ and decimated to $200 \mu s$. In this setting, the sampling frequency is five times higher

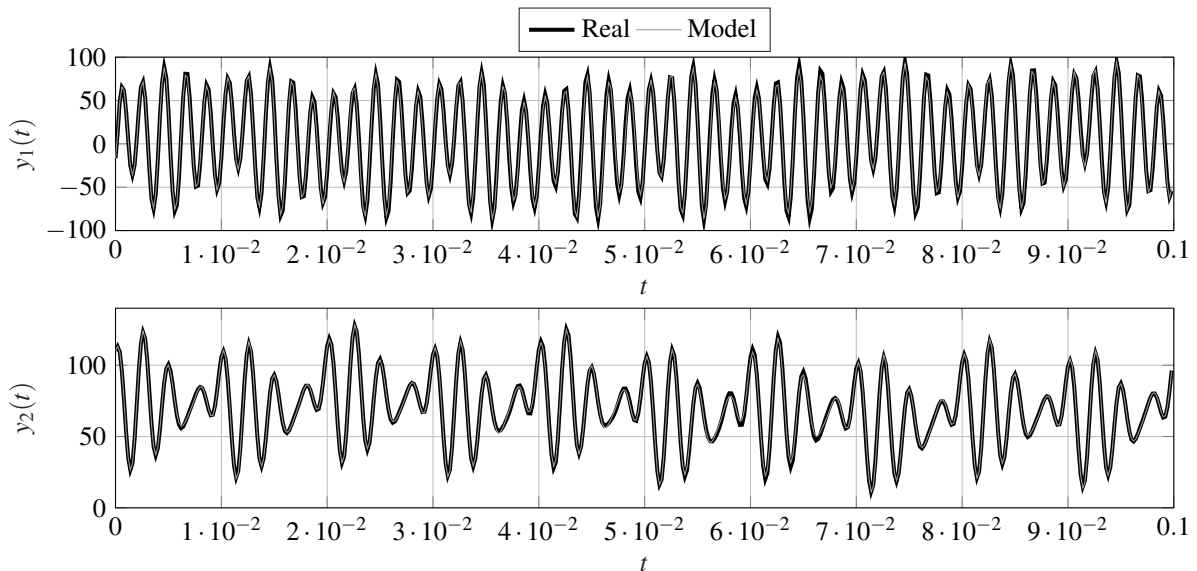


Fig. 5. Real data and model outputs in free-run simulation for the estimation and validation phases.

than the Nyquist sampling frequency one should need to represent a signal with 500 Hz (highest frequency in the input signal). The acquired data was then split in estimation and validation datasets, with 250 samples each.

We performed numerical simulations using MATLAB software by varying the order of the models $n_{y_i} = n_{u_j} = 1, 2, \dots, 10$. The results in terms of R^2 improve together with increasing orders on the lagged inputs and output and with $n_{y_i} = n_{u_j} = 4$ this metric is close to unity for all measured outputs. The statistical tests in (6) however are not satisfied until $n_{y_i} = n_{u_j} = 9$, which is the solution which will be depicted in the following.

In Fig. 4 we show the correlation based tests as in (6). It is possible to see that the model is statistically valid with respect to the tests in (6). This shows that the system dynamics present in the data has been adequately captured by the model. In Fig. 5 we plot the results in terms of the model responses in FR simulation in the estimation and validation data. It is possible to see that the model is accurate and able to adequately represent the micromanipulator dynamics.

V. CONCLUSIONS

We showed the effective application of nonlinear black-box system identification to model a 2-DOF piezoelectric micromanipulator with real acquired data. The results showed that the model was able to adequately capture the cross-coupled dynamics of the system even at higher frequency rates. The goal was to explore the adherence of the model to the data towards more effective control design at higher frequency ranges. This will permit rapid and precise micromanipulation, through the use of model-based control design or model feedback in the case of sensorless applications.

In future works we will aim at different nonlinear model structures, such as NARMAX [31] and novel approaches, such as nonlinear difference equation with moving average

noise [32], in order to assess the best structure for the 2-DOF micromanipulator system. Moreover, another use of the model would be to enhance feedback in micropositioning, as avoiding the use of sensors represents a major gain in cost and the possibility to embed such micromanipulators in specific applications. A future research endeavour will be to assess the performance of the above mentioned model classes to perform feedback. In this context, the use of standard and advanced control techniques for such models will also be pursued, such as evolutionary multiobjective proportional-integral-derivative, robust, optimal and model predictive controllers [33]-[36]. The design of the excitation signal for the case of micromanipulators should be further studied. The general guidelines for designing excitation signals for nonlinear identification is to use prior knowledge about the system at hand according to the intended use for the model, excite both the bandwidth of interest and the full amplitude range and set length and distribution of the dataset [29], [37]. In the specific case of piezoelectric micromanipulators, we are interested in acquiring both the dynamics and the cross-coupled hysteretic behavior of the system and a thorough comparison of excitation signals for the present case is lacking. Another approach which deserves attention in the future is the application of gray-box modeling, as we illustrate in the following examples. The model structure of hysteresis may be estimated in conjunction with black-box approaches, so that the later is able to capture what is left of dynamics in the former, what may leverage the accuracy of the models as a whole. The second suggestion is to use the knowledge of the hysteretic behavior of the model as a complimentary metric of the residuals, a problem that can be solved with a multiobjective optimization approach. Being so, there could be two different data-sets which are used in the training procedure, where the multiobjective approach tries to minimize the error. In [38] the authors use

the knowledge about the static curve of the system to be optimized together with the dynamic data in a multiobjective problem.

ACKNOWLEDGMENTS

This work has been partially supported by project no. 88887.163347/2018-00 from CAPES (Coordination for the Improvement of Higher Education Personnel – Brazilian Government).

REFERENCES

- [1] J. Agnus, N. Chaillet, C. Clévy, S. Dembélé, M. Gauthier, Y. Haddab, G. Laurent, P. Lutz, N. Piat, K. Rabenorosoa, M. Rakotondrabe, and B. Tamadazte, "Robotic microassembly and micromanipulation at femto-st," *Journal of Micro-Bio Robotics*, vol. 8, no. 2, pp. 91–106, 2013.
- [2] T. E. Pengwang, K. Rabenorosoa, M. Rakotondrabe, and N. Andreff, "Scanning micromirror platform based on memstechnology for medical applications," *MDPI Micromachines*, 2016.
- [3] S. Devasia, E. Eleftheriou, and S. Moheimani, "A survey of control issues in nanopositioning," *IEEE Transactions on Control Systems Technology*, vol. 15, no. 5, pp. 802–823, 2007.
- [4] M. Rakotondrabe, *Smart Materials-Based Actuators at the Micro/Nano-Scale: Characterization, Control, and Applications*. New York, USA: Springer, 2013.
- [5] M. Rakotondrabe and I. Ivan, "Development and dynamic modeling of a new hybrid thermopiezoelectric microactuator," *IEEE Transactions on Robotics*, vol. 26, no. 6, pp. 1077–1085, 2010.
- [6] Y. Haddab, N. Chaillet, and A. Bourjault, "A microgripper using smart piezoelectric actuators," in *IEEE/RSJ International Conference on Intelligent Robots and Systems*, vol. 1, 2000, pp. 659–664 vol.1.
- [7] M. Rakotondrabe, K. Rabenorosoa, J. Agnus, and N. Chaillet, "Robust feedforward-feedback control of a nonlinear and oscillating 2-DOF piezocantilever," *IEEE Transactions on Automation Science and Engineering*, vol. 8, no. 3, pp. 506–519, 2011.
- [8] J.-A. Escareno, M. Rakotondrabe, and D. Habineza, "Backstepping-based robust-adaptive control of a nonlinear 2-DOF piezoactuator," *Control Engineering Practice*, vol. 41, pp. 57–71, 2015.
- [9] D. Habineza, M. Rakotondrabe, and Y. Le Gorrec, "Bouc-wen modeling and feedforward control of multivariable hysteresis in piezoelectric systems: Application to a 3-DOF piezotube scanner," *IEEE Transactions on Control Systems Technology*, vol. 23, no. 5, pp. 1797–1806, 2015.
- [10] J. Escareno, J. Abadie, E. Piat, and M. Rakotondrabe, "Micropositioning of 2DOF piezocantilever: LKF compensation of parasitic disturbances," in *IEEE/RSJ International Conference on Intelligent Robots and Systems*, Hamburg, Germany, 2015, pp. 6026–6032.
- [11] D. Habineza, M. Rakotondrabe, and Y. Le Gorrec, "Simultaneous suppression of badly damped vibrations and cross-couplings in a 2-DOF piezoelectric actuator by using feedforward standard hinf approach," in *SPIE - Sensing Technology+Applications; Sensors for Next Generation Robots conference*, vol. 9494, Baltimore Maryland USA, 2015, pp. 9494–29.
- [12] Y. A. Hamidi and M. Rakotondrabe, "Multi-mode vibration suppression in 2-dof piezoelectric systems using zero placement input shaping technique," in *SPIE - Sensing Technology+Applications; Sensors for Next Generation Robots conference*, vol. 9494, Baltimore Maryland USA, 2015, pp. 9494–27.
- [13] M. Rakotondrabe, "Modeling and compensation of multivariable creep in multi-dof piezoelectric actuators," in *IEEE International Conference on Robotics and Automation*, 2012, pp. 4577–4581.
- [14] M. Rakotondrabe, Y. Haddab, and P. Lutz, "Quadrilateral modelling and robust control of a nonlinear piezoelectric cantilever," *IEEE Transactions on Control Systems Technology*, vol. 17, no. 3, pp. 528–539, 2009.
- [15] M. Rakotondrabe, "Multivariable classical prandtl-ishlinskii hysteresis modeling and compensation and sensorless control of a nonlinear 2-dof piezoactuator," *Nonlinear Dynamics*, pp. 1–19, 2017.
- [16] J. Sjöberg, Q. Zhang, L. Ljung, A. Benveniste, B. Delyon, P.-Y. Glorennec, H. Hjalmarsson, and A. Juditsky, "Nonlinear black-box modeling in system identification: a unified overview," *Automatica*, vol. 31, no. 12, pp. 1691–1724, 1995.
- [17] R. Johansson, A. Robertsson, K. Nilsson, and M. Verhaegen, "State-space system identification of robot manipulator dynamics," *Mechatronics*, vol. 10, no. 3, pp. 403–418, 2000.
- [18] M. Ostring, S. Gunnarsson, and M. Norrlof, "Closed-loop identification of an industrial robot containing flexibilities," *Control Engineering Practice*, vol. 11, no. 3, pp. 291 – 300, 2003.
- [19] R. D. Al-Dabbagh, A. Kinsheel, S. Mekhilef, M. S. Baba, and S. Shamsirband, "System identification and control of robot manipulator based on fuzzy adaptive differential evolution algorithm," *Advances in Engineering Software*, vol. 78, pp. 60 – 66, 2014.
- [20] J. Wu, J. Wang, and Z. You, "An overview of dynamic parameter identification of robots," *Robotics and Computer-Integrated Manufacturing*, vol. 26, no. 5, pp. 414 – 419, 2010.
- [21] Y. Wang and S. Boyd, "Fast model predictive control using online optimization," *IEEE Transactions on Control Systems Technology*, vol. 18, no. 2, pp. 267–278, 2010.
- [22] J. L. Jerez, P. J. Goulart, S. Richter, G. Constantinides, E. C. Kerrigan, and M. Morari, "Embedded online optimization for model predictive control at megahertz rates," *IEEE Transactions on Automatic Control*, vol. 59, no. 12, pp. 3238–3251, 2014.
- [23] H. V. H. Ayala, D. Habineza, M. Rakotondrabe, C. E. Klein, and L. S. Coelho, "Nonlinear black-box system identification through neural networks of a hysteretic piezoelectric robotic micromanipulator," in *17th IFAC Symposium on System Identification*. Beijing, China: IFAC, 2015.
- [24] M. Rakotondrabe, M. Janaideh, A. Bienaim, and Q. Xu, *Smart materials-based actuators at the micro/nano-scale*. Springer, 2013.
- [25] R. Babuška and H. Verbruggen, "Neuro-fuzzy methods for nonlinear system identification," *Annual Reviews in Control*, vol. 27, no. 1, pp. 73–85, 2003.
- [26] R. Haber and H. Unbehauen, "Structure identification of nonlinear dynamic systems—a survey on input/output approaches," *Automatica*, vol. 26, no. 4, pp. 651–677, 1990.
- [27] S. Billings and W. S. F. Voon, "Structure detection and model validity tests in the identification of nonlinear systems," *IEE Proceedings Pt. D: Control Theory and Applications*, vol. 130, no. 4, pp. 193–199, 1983.
- [28] S. Billings, H. Jamaluddin, and S. Chen, "Properties of neural networks with applications to modelling non-linear dynamical systems," *International Journal of Control*, vol. 55, no. 1, pp. 193–224, 1992.
- [29] S. A. Billings, *Nonlinear system identification: NARMAX methods in the time, frequency, and spatio-temporal domains*. West Sussex, United Kingdom: John Wiley & Sons Ltd., 2013.
- [30] R. Pintelon and J. Schoukens, *System identification: a frequency domain approach*, 2nd ed. Piscataway, NJ: John Wiley & Sons, 2012.
- [31] S. Chen and S. A. Billings, "Representations of non-linear systems: the NARMAX model," *International Journal of Control*, vol. 49, no. 3, pp. 1013–1032, 1989.
- [32] B. Zhang and S. Billings, "Identification of continuous-time nonlinear systems: The nonlinear difference equation with moving average noise (NDEMA) framework," *Mechanical Systems and Signal Processing*, vol. 60–61, pp. 810 – 835, 2015.
- [33] D. Mayne, J. Rawlings, C. Rao, and P. Scokaert, "Constrained model predictive control: Stability and optimality," *Automatica*, vol. 36, no. 6, pp. 789–814, 2000.
- [34] G. Reynoso-Meza, X. Blasco, J. Sanchis, and M. Martínez, "Controller tuning using evolutionary multi-objective optimisation: Current trends and applications," *Control Engineering Practice*, vol. 28, pp. 58 – 73, 2014.
- [35] J. H. Lee, "From robust model predictive control to stochastic optimal control and approximate dynamic programming: A perspective gained from a personal journey," *Computers & Chemical Engineering*, vol. 70, pp. 114 – 121, 2014.
- [36] M. G. Forbes, R. S. Patwardhan, H. Hamadah, and R. B. Gopaluni, "Model predictive control in industry: Challenges and opportunities," in *9th IFAC Symposium on Advanced Control of Chemical Processes*, vol. 48, no. 8, Whistler, Canada, 2015, pp. 531– 538.
- [37] O. Nelles, *Nonlinear system identification: from classical approaches to neural networks and fuzzy models*. Berlin: Springer-Verlag Berlin Heidelberg GmbH, 2001.
- [38] B. H. Barbosa, L. A. Aguirre, C. B. Martinez, and A. P. Braga, "Black and gray-box identification of a hydraulic pumping system," *IEEE Transactions on Control Systems Technology*, vol. 19, no. 2, pp. 398–406, 2011.